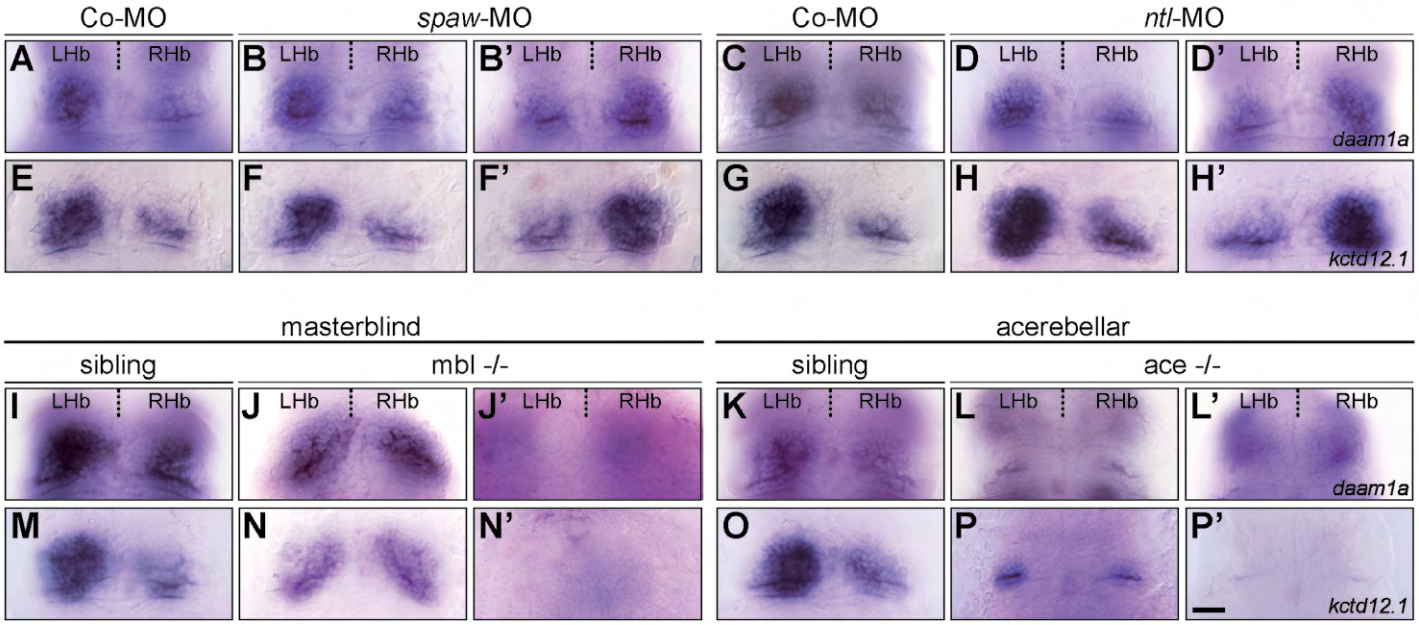

Fig. S1. Habenular expression of daam1a and kcdt12.1 in embryos with affected habenular asymmetry. (**A**,**C**,**I**,**K**) Habenular expression of daam1a in embryos injected with Co-MO (A,C) and in siblings of masterblind (mbl) (I) and acerebellar (ace) (K) mutants. (**E**,**G**,**M**,**O**) Habenular expression of kcdt12.1 in embryos injected with Co-MO (E,G) and in siblings of mbl (M) and ace (O) mutants. (**B**,**B′**,**F**,**F′**) Injection of spaw-MO results in randomised laterality of habenular daam1a (B,B′) and kcdt12.1 (F,F′) asymmetric expression. (**D**,**D′**,**H**,**H′**) Injection of ntl-MO results in randomised laterality of habenular daam1a (D,D′) and kcdt12.1 (H,H′) asymmetric expression. (**J**,**J′**,**N**,**N′**) $mbl^{-/-}$ mutants show symmetric expression of daam1a (J) and kcdt12.1 (N), with both sides showing levels similar to the right Hb of controls; some embryos also show absence of expression (J′,N′). (**L**,**L′**,**P**,**P′**) $ace^{-/-}$ mutants show symmetric expression of daam1a (L) and kcdt12.1 (P), with both sides showing levels similar to the right Hb of controls; some embryos also show absence of expression (L′,P′). The relative contribution of the different phenotypes is given in Table 1. Images correspond to dorsal views of the habenular region at 96 hpf, with anterior to the top. Scale bar, 20 μm.

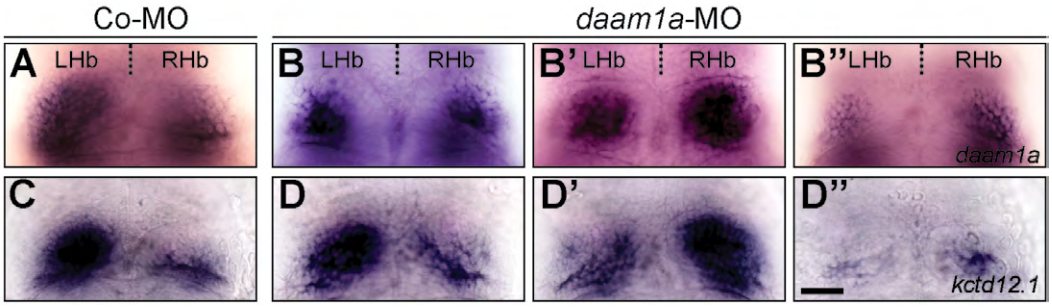

Fig. S2. Habenular expression of *daam1a* and kctd12.1 after Daam1a knock-down. (**A**,**C**) Expression of daam1a (A) and kcdt12.1 (C) in control embryos, revealing the enlarged asymmetric domain of the left Hb. (**B-B′′**) Global knock down of Daam1a results in equal proportions of asymmetric left-sided (B), asymmetric right-sided (B′), and bilateral-right symmetric (B′′) expression of daam1a. (**D-D′′**) Global knock down of Daam1a leads to equal proportions of asymmetric left-sided (D), asymmetric right-sided (D′), and bilateral-right symmetric (D′′) expression of kcdt12.1. The relative contributions of the different phenotypes are given in Table 2. Images correspond to dorsal views of the habenular region at 96 hpf, with anterior to the top. Scale bar, 20 μm.

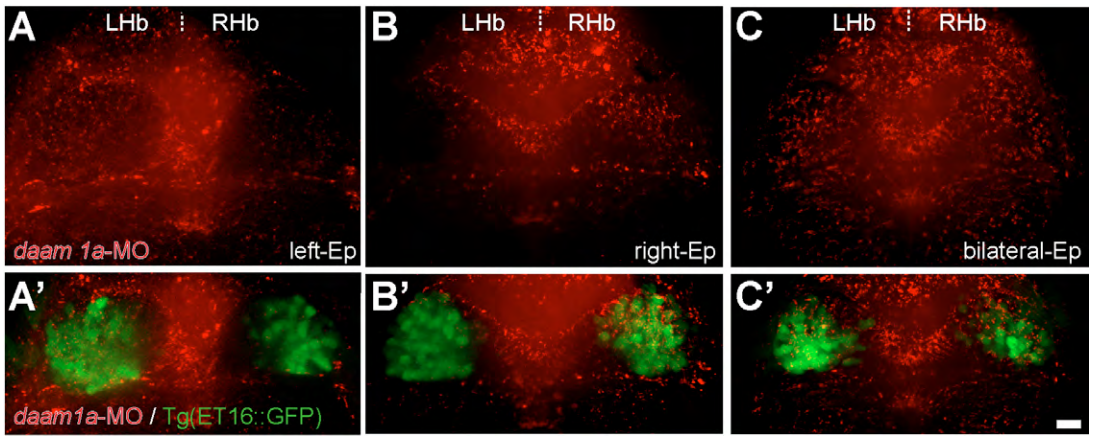

Fig. S3. Efficiency of daam1a-MO local electroporation (Ep) in the habenular region. (**A-C′**) Distribution of lissamine-tagged daam1a-MO (red) locally electroporated into the left (A,A′), right (B,B′) and bilateral (C,C′) habenular regions (green) of Tg(ET16::GFP) embryos. Images correspond to dorsal views of maximum intensity z-stack confocal projections, with anterior to the top. Scale bar, 20 µm.

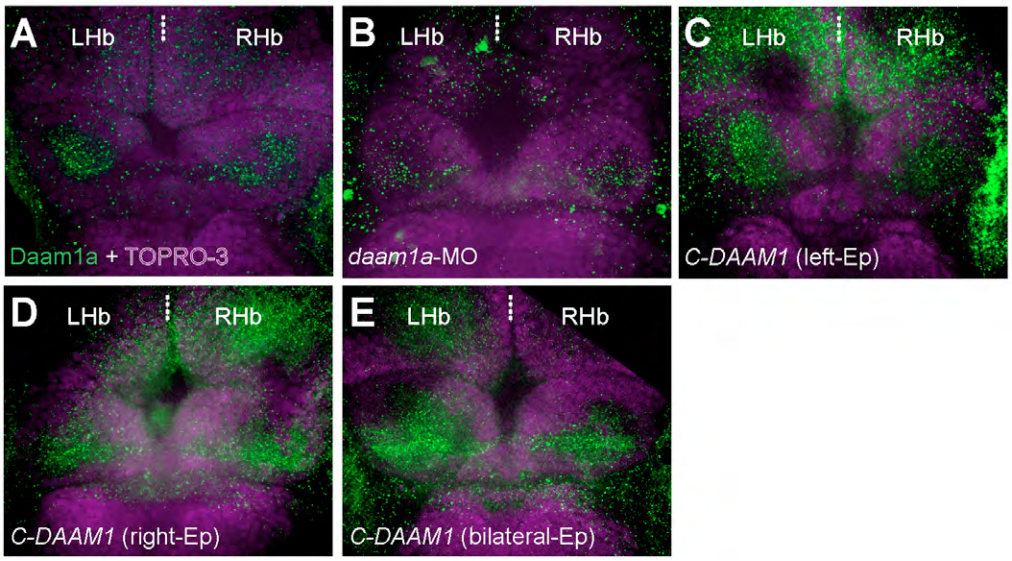

Fig. S4. Changes in the relative levels of the endogenous Daam1a protein after local electroporation (Ep). (**A**) The Hb of control embryos labelled through indirect immunofluorescence against Daam1a (green) and counter stained with TO-PRO-3 to delineate the cellular context of the Hb (purple) showed a distinct punctate expression of Daam1a in the habenular neuropil, larger on the left compared to the right side at 96 hpf. (**B**) The Hb of embryos subjected to left-sided local electroporation of daam1a-MO show decreased levels of Daam1a expression at 96 hpf, primarily on the left Hb. (**C**) The Hb of embryos subjected to left-sided local electroporation of *C-DAAM1* showed increased levels of Daam1a expression in the left Hb at 96 hpf. (**D**) The Hb of embryos after right-sided local electroporation of *C-DAAM1* showed increase expression levels of Daam1a in the right Hb at 96 hpf, compared to controls. (**E**) The Hb of embryos subjected to bilateral local electroporation of *C-DAAM1* showed increased levels of Daam1a expression in both left and right Hb at 96 hpf. Images correspond to dorsal views of maximum intensity z-stack confocal projections, with anterior to the top. Scale bar, 20 µm.

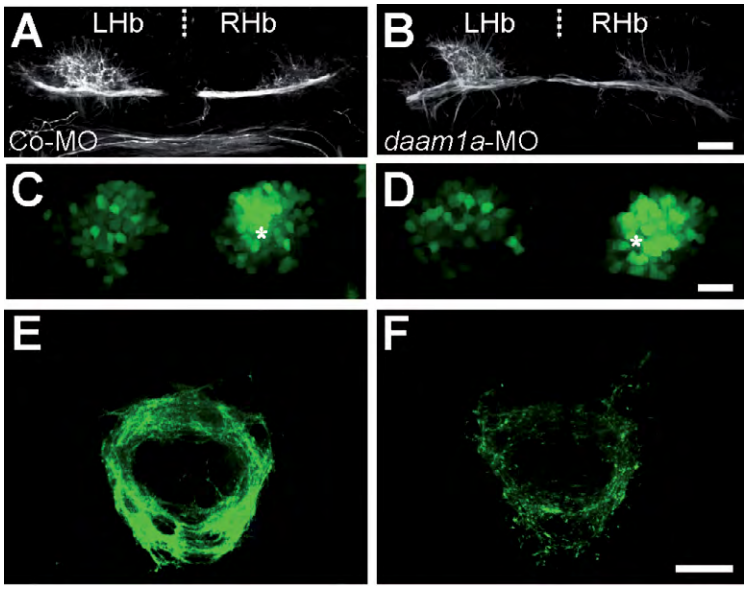

Fig. S5. Bilateral electroporation of daam1a-MO induces defects in neuropil formation and IPN connectivity. (**A-F**) Dorsal views of maximum intensity z-stack confocal projections of the habenular region (A-D) and IPN (E,F) in Tg(pou4f1-hsp70l:GFP) embryos at 4.5 dpf, with anterior to the top. The habenular neuropil was immunostained against acetylated α-tubulin (A,B, white), while the soma (C,D) and efferent projections (E,F) of dorsal habenular neurons expressing pou4f1-hsp70l:GFP were detected in vivo (green). Each column corresponds to a different condition of local electroporation: control-MO (left) and daam1a-MO (right). Asterisks in C and D indicate the enlarged cellular domain of the Hb expressing the pou4f1-hsp70l:GFP transgene. Scale bar, 20µm.

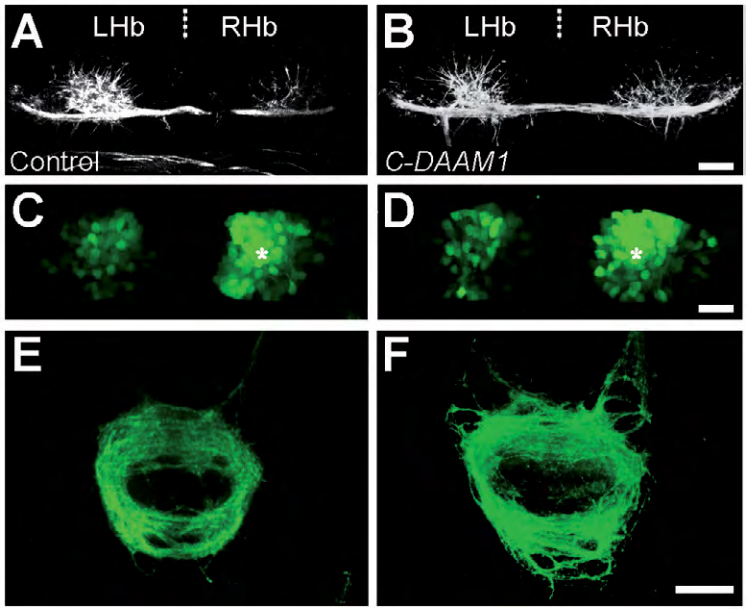

Fig. S6. Local electroporation of *C-DAAM1* in the right habenular region induces increased axonal efferent connectivity to the IPN, without affecting habenular neuropil. (**A-F**) Dorsal views of maximum intensity z-stack confocal projections of the habenular region (A-D) and IPN (E,F) in Tg(pou4f1-hsp70l:GFP) embryos at 4.5 dpf, with anterior to the top. The habenular neuropil was immunostained against acetylated α-tubulin (A,B, white), while the soma (C,D) and efferent projections (E,F) of dorsal habenular neurons expressing pou4f1-hsp70l:GFP were detected in vivo (green). Each column corresponds to a different condition of local electroporation: control plasmid (left) and *pcDNA-C-DAAM1-HA* (right). Asterisks in C and D indicate the enlarged cellular domain of the Hb expressing the pou4f1-hsp70l:GFP transgene. Scale bar, 20µm.